

# Fe<sub>2</sub>(SO<sub>4</sub>)<sub>3</sub> as a Binary Oxidant and Dopant to Thin Polyaniline Nanowires with High Conductivity

Hangjun Ding,<sup>†</sup> Yunze Long,<sup>‡</sup> Jiaoyan Shen,<sup>§</sup> and Meixiang Wan<sup>\*,||</sup>

School of Materials Science and Engineering, University of Science and Technology Beijing, Beijing 100083, P. R. China, College of Physics Science, Qingdao University, Qingdao 266071, P. R. China, School of Mathematics and Physics, Suzhou University of Science and Technology, Suzhou 215011, P. R. China, and Institute of Chemistry, Chinese Academy of Sciences, Beijing 100190, P. R. China

Received: September 13, 2009; Revised Manuscript Received: November 11, 2009

This article exposes a facial approach to self-assemble polyaniline (PANI) nanowires with thin diameter ( $\sim 10$  nm) and high room-temperature conductivity ( $\sim 10^0$  S/cm) by using Fe<sub>2</sub>(SO<sub>4</sub>)<sub>3</sub> as a binary oxidant and dopant. The new method not only saves hard templates and postprocess of template removal but also simplifies the reagent. Formation yield, diameter, and room-temperature conductivity of the nanowires are affected by the molar ratios of Fe<sub>2</sub>(SO<sub>4</sub>)<sub>3</sub> to aniline. The low redox potential of Fe<sub>2</sub>(SO<sub>4</sub>)<sub>3</sub> not only results in a thinner diameter and higher room-temperature conductivity ( $10^0$  S/cm) of the nanowires but also shows a much weaker temperature dependence of resistivity and smaller characteristic Mott temperature ( $T_0 = 2.5 \times 10^3$  K).

## 1. Introduction

One-dimensional (1D) conducting polymer nanostructures (e.g., nanotubes, nanofibers, or nanowires) with a diameter of 1–100 nm have recently received great attention in nanoscience and nanotechnology because of the combination of metal-like conductivity, reversible properties controlled by a novel doping/dedoping process, and intrinsic characteristics of the nanomaterials, leading to the promising applications in molecular and nanodevices.<sup>1</sup> As is well-known, the size, surface, and quantum effect of the nanomaterials result in the different physical properties from their bulk materials. Some research groups<sup>2–6</sup> have reported the size effect on the conductivity of the conducting polymer nanostructures, which shows the conductivity increases with a decrease of the size, and recently, the size effect on conductivity has been directly demonstrated by measurement of the room-temperature conductivity on a single nanotube/wire using a four-probe method.<sup>7</sup> The surface effect caused by small size<sup>8,9</sup> on the sensitivity of the gas sensors made of PANI nanofibers has also been observed.<sup>10,11</sup> From the viewpoint of application of conducting polymer-based nanodevices, well-controlled nanoscaled 1D nanotubes or nanowires are desired.

To our best knowledge, a diameter of the conducting polymer nanofibers as thin as 3 nm has been prepared by using MCM-41 as the template.<sup>12</sup> Although a well-controlled diameter of conducting polymer nanostructures can be achieved by the porous size of the membrane as the hard template, the postprocess of template removal not only leads to a complex preparation process but also results in destroying the morphology of the resultant nanostructures. Soft-template methods, such as surfactant-assisted polymerization,<sup>13</sup> interfacial polymerization,<sup>14</sup> template-free method,<sup>15</sup> “seeding” method,<sup>16</sup> and dilute polymerization,<sup>17</sup> have also been developed to synthesize 1D nanostructures of conducting polymers. The diameter of soft-template

synthesized nanostructures can be adjusted by the dopant structure and polymerization conditions.<sup>8</sup> Up to date, however, the diameters of most nanofibers or nanotubes prepared by a soft-template method are larger than 50 nm. As a result, developing facial approaches to thin 1D nanotubes/nanofibers or nanowires (e.g., less than 10 nm) of the conducting polymers are desired.

Among the family of conjugated conducting polymers, polyaniline (PANI) has been most extensively studied because of its high conductivity, excellent environmental stability, simple synthesis, and controllable chemical and physical properties by the oxidation and protonation state. Trchova et al.<sup>19</sup> recently reported that PANI nanotubes could be directly oxidized by ammonium persulfate ((NH<sub>4</sub>)<sub>2</sub>S<sub>2</sub>O<sub>8</sub>, APS) in water without adding acid. The trick is that reaction of aniline with APS produces H<sub>2</sub>SO<sub>4</sub>, which can be used as the dopant of PANI.<sup>20</sup> Our group also successfully synthesized PANI nanotubes<sup>21</sup> and hollow microspheres of PANI derivatives<sup>22</sup> by using APS or FeCl<sub>3</sub> as both the oxidant and dopant at the same time, respectively. Moreover, well-controlled diameter of the PANI nanofibers could be directly oxidized by various oxidants.<sup>23</sup> The new finding exposed a facial approach to thin nanostructures of conducting polymer by using an oxidant with a low redox potential. However, the effect factors and the electronic transport properties of the thin resultant nanostructures were not studied. As shown in Scheme 1, Fe<sub>2</sub>(SO<sub>4</sub>)<sub>3</sub> is an acidic salt that can be hydrolyzed to produce a proton (H<sup>+</sup>) in aqueous solution, indicating that Fe<sub>2</sub>(SO<sub>4</sub>)<sub>3</sub> can serve as a binary oxidant and dopant. Moreover, the redox potential of Fe<sub>2</sub>(SO<sub>4</sub>)<sub>3</sub> is about 0.68 eV, which is lower than that of APS (2.05 V).<sup>24</sup> These characteristics of Fe<sub>2</sub>(SO<sub>4</sub>)<sub>3</sub> might contribute to new properties of the PANI nanostructures when it is used as a binary oxidant and dopant.

Herein, we reported PANI nanowires with a diameter of  $\sim 10$  nm and room-temperature conductivity as high as  $10^0$  S/cm can be template-free synthesized by using Fe<sub>2</sub>(SO<sub>4</sub>)<sub>3</sub> as a binary oxidant and dopant. The function of the binary oxidant and dopant of Fe<sub>2</sub>(SO<sub>4</sub>)<sub>3</sub> in the nanowires has been demonstrated

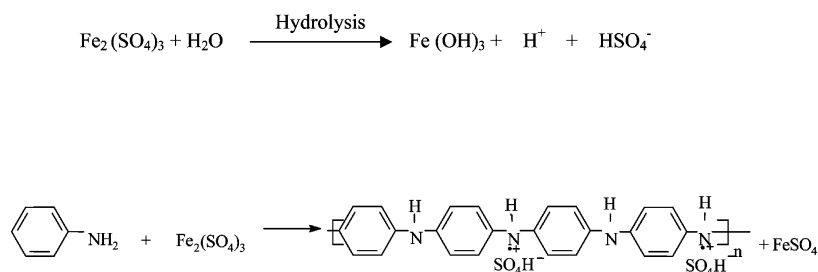
<sup>†</sup> University of Science and Technology Beijing.

<sup>‡</sup> Qingdao University.

<sup>§</sup> Suzhou University of Science and Technology.

<sup>||</sup> Chinese Academy of Sciences.

## SCHEME 1



by structural characterizations. The electrical and electronic transport properties of the nanowires were measured by a four-probe method.

## 2. Results and Discussion

**2.1. Morphology and Self-Assembly Formation Mechanism.** The PANI nanowires were self-assembled by using  $\text{Fe}_2(\text{SO}_4)_3$  as a binary oxidant and dopant. The typical synthesis process of the nanowires is as follows: 0.2 mL (2 mmol) of aniline was dissolved in 10 mL of deionized water with magnetic stirring at room temperature for 0.5 h. The precooled 10 mL of aqueous  $\text{Fe}_2(\text{SO}_4)_3$  (6 mmol) was added to the above solution. The mixture was allowed to react at 0–5 °C for 15 h. The PANI precipitate was washed with water, methanol, and ether several times, respectively. Finally, the product was dried in a vacuum at room temperature for 24 h.

It is found that formation yield, morphology, and aggregation of the resultant PANI are affected by the molar ratio of  $\text{Fe}_2(\text{SO}_4)_3$  to aniline (represented by  $[\text{Fe}_2(\text{SO}_4)_3]/[\text{An}]$  ratios), as shown in Figure 1. As the  $[\text{Fe}_2(\text{SO}_4)_3]/[\text{An}]$  ratio is less than 2:1, for instance, irregular PANI granules are observed (see Figure 1a). As the  $[\text{Fe}_2(\text{SO}_4)_3]/[\text{An}]$  ratio increased to 3:1 or 5:1, uniform nanowires of ~10 nm in diameter (formation yield ~100%) were observed (see Figure 1b and c). As the  $[\text{Fe}_2(\text{SO}_4)_3]/[\text{An}]$  ratio became larger than 10:1, the diameter of the nanowires slightly increased from ~10 to 20 nm, and aggregated together to form flakes (see Figure 1d). On the basis of the above results, the optimal  $[\text{Fe}_2(\text{SO}_4)_3]/[\text{An}]$  ratio between 3:1 and 5:1 is found to self-assemble thin nanowires (~10 nm) with high formation

yield, and TEM showed the nanowires are solid (see Figure 2b). For comparison, the PANI nanostructures were also synthesized by using APS as both an oxidant and dopant using

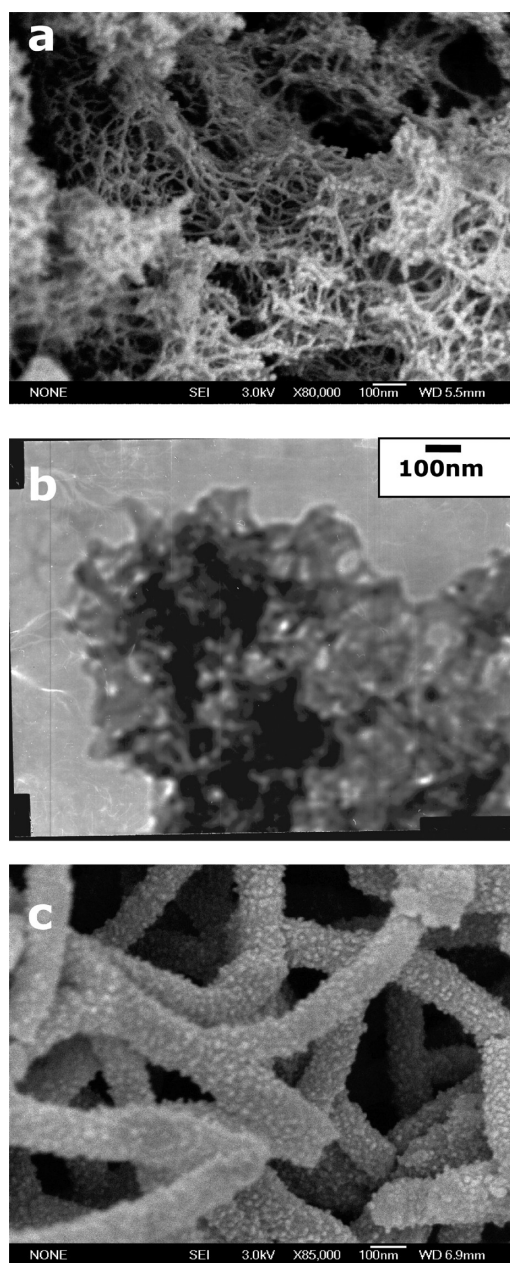


**Figure 2.** Influence of the redox potential of the oxidant on the morphology and diameter of the PANI nanowires: SEM (a) and TEM (b) of the nanowires oxidized by  $\text{Fe}_2(\text{SO}_4)_3$ , respectively, and (c) SEM of the nanowires oxidized by APS. Other reaction conditions:  $[\text{An}] = 0.1 \text{ M}$ ;  $[\text{APS}]/[\text{An}] = 1:1$ ;  $[\text{Fe}_2(\text{SO}_4)_3]/[\text{An}] = 3:1$ ; reaction time, 15 h; reaction temperature, 0–5 °C.

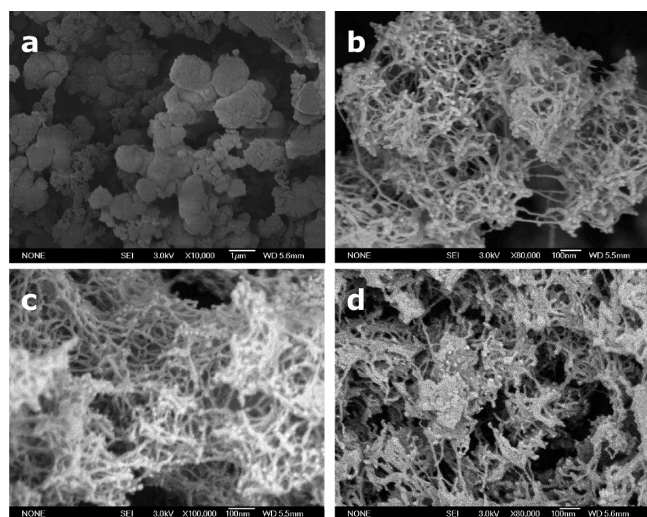


**Figure 1.** Effect of the  $[\text{Fe}_2(\text{SO}_4)_3]/[\text{An}]$  ratios on the morphology of the PANI nanowires: (a)  $[\text{Fe}_2(\text{SO}_4)_3]/[\text{An}] = 0.5:1$ ; (b)  $[\text{Fe}_2(\text{SO}_4)_3]/[\text{An}] = 3:1$ ; (c)  $[\text{Fe}_2(\text{SO}_4)_3]/[\text{An}] = 5:1$ ; (d)  $[\text{Fe}_2(\text{SO}_4)_3]/[\text{An}] = 10:1$ . Other reaction conditions:  $[\text{An}] = 0.1 \text{ M}$ ; reaction time, 15 h; reaction temperature, 0–5 °C.

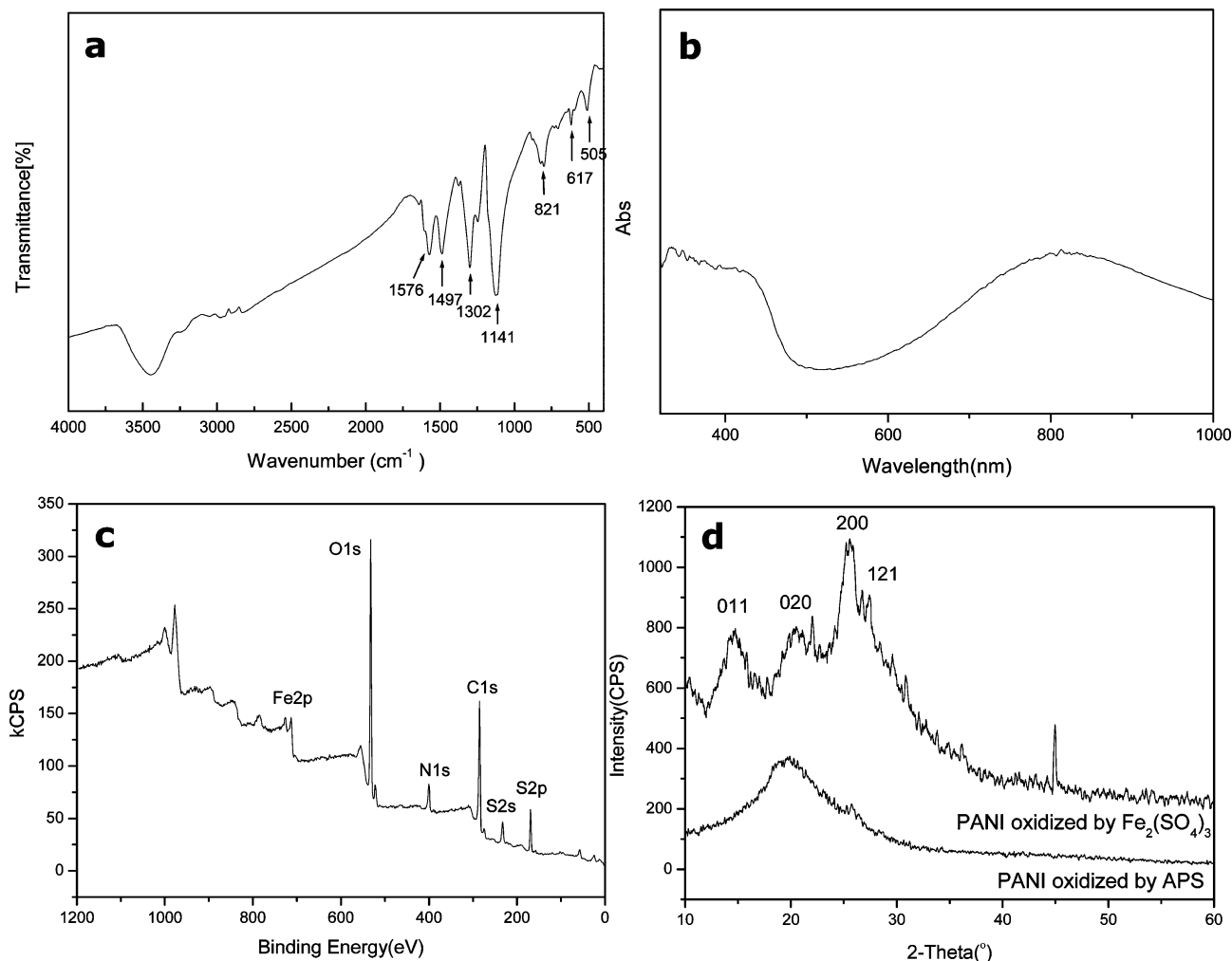


**Figure 3.** Molecular structure of the PANI nanowires characterized by (a) UV–visible spectra dissolved in *m*-cresol, (b) infrared spectra, (c) XPS analysis, and (d) XRD patterns oxidized by  $\text{Fe}_2(\text{SO}_4)_3$  and APS as the binary oxidant and dopant. Other reaction conditions:  $[\text{An}] = 0.1 \text{ M}$ ;  $[\text{Fe}_2(\text{SO}_4)_3]/[\text{An}] = 3:1$ ;  $[\text{APS}]/[\text{An}] = 1:1$ ; reaction time, 15 h; reaction temperature, 0–5 °C.

the same synthesis process. The difference in morphology and diameter between them is shown in Figure 2. When  $\text{Fe}_2(\text{SO}_4)_3$  is replaced by APS, it is found that the morphology is unchanged, but the diameter is estimated to be about 150 nm, which is enhanced by 15 times as compared with that of the PANI nanowires oxidized by  $\text{Fe}_2(\text{SO}_4)_3$ , due to the redox potential of APS ( $E_{\text{ox}} = 2.05 \text{ V}$ )<sup>24</sup> being higher than that of  $\text{Fe}_2(\text{SO}_4)_3$  ( $E_{\text{ox}} = 0.68 \text{ V}$ ).

Aniline monomer can be regarded as an amphiphile molecule because of its hydrophobic group of benzene ring and hydrophilic  $-\text{NH}_2$  group. On the basis of our previous results,<sup>25</sup> micelles composed of aniline monomer or aniline salts in aqueous solution serve as the soft templates in the formation of the PANI nanostructures. Since  $\text{Fe}_2(\text{SO}_4)_3$  is hydrophilic, the polymerization took place only at the micelle/water interface and the growth of the nanowires was controlled by polymerization and elongation process.<sup>26,27</sup> However, it is expected that formation and competition of the two above-mentioned micelles are affected by the  $[\text{Fe}_2(\text{SO}_4)_3]/[\text{An}]$  ratios, resulting in an effect of the  $[\text{Fe}_2(\text{SO}_4)_3]/[\text{An}]$  ratios on the diameter, morphology, and aggregation of the resultant PANI. This is consistent with our observations, as shown in Figure 1.

**2.2. Structural Characterization.** It has been demonstrated that the PANI nanowires are identical to the emeraldine salt form of PANI (i.e., conducting state) by means of UV–visible and FTIR absorption, room-temperature conductivity measured

by the four-probe method, doping degree measured by X-ray photoelectric spectrometry (XPS), and elemental analysis. As shown in Figure 3a, UV–visible absorption spectra of the nanowires dissolved in *m*-cresol solvent have two bands at 420 and 800 nm with a long tail that are characteristic of the emeraldine salt form of PANI.<sup>28</sup> Moreover, all character bands of PANI chains, such as C=C stretching deformation of quinoid at  $1576 \text{ cm}^{-1}$ , benzene rings at  $1497 \text{ cm}^{-1}$ , the C–N stretching of secondary aromatic amine at  $1302 \text{ cm}^{-1}$ , the aromatic C–H in-plane bending at  $1141 \text{ cm}^{-1}$ , and the out-of-plane deformation of C–H in the 1,4-disubstituted benzene ring at 821 and 505  $\text{cm}^{-1}$  are observed (see Figure 3b).<sup>29</sup> Especially, the band at 617 and  $1141 \text{ cm}^{-1}$  ascribed to the absorption of S–O group<sup>30</sup> is also observed, indicating the  $-\text{HSO}_4^-$  are incorporated into the polymeric chain of PANI as counteranions. It was noted that the influence of the  $[\text{Fe}_2(\text{SO}_4)_3]/[\text{An}]$  ratios on the polymeric chain and electronic structure of the nanowires can be negligible. XPS analysis released that the nanowires are mainly composed of C, N, and S elements (see Figure 3c) and the doping degree assigned as  $[\text{N}^+]/[\text{N}]$  ratios is ca. 0.36, which is consistent with the S/N ratio of 0.38 calculated by element analysis. This is also consistent with a high conductivity of  $10^5 \text{ S/cm}$ , as measured by the four-probe method. The above results proved that  $\text{Fe}_2(\text{SO}_4)_3$  served as a binary oxidant and dopant, and  $-\text{HSO}_4^-$  anion is incorporated into the PANI main chain as the counteranion.



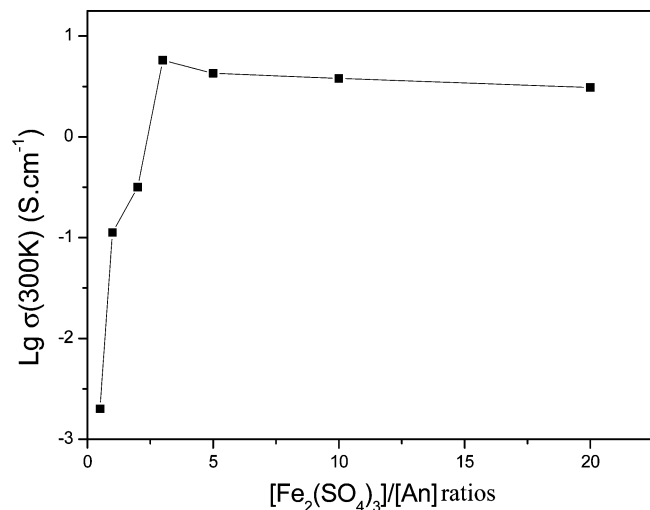


**Figure 4.** Effect of the  $[\text{Fe}_2(\text{SO}_4)_3]/[\text{An}]$  ratios on room-temperature conductivity of the PANI nanowires measured by a four-probe method.

XRD of the nanowires shows four peaks centered at  $2\theta = 14.7, 20.4, 25,$  and  $26.7$  (see Figure 3d) that are consistent with the monoclinic space group  $P2_1$ .<sup>31</sup> On the other hand, the nanowires oxidized by APS are amorphous, which is in agreement with previously reports.<sup>32</sup> On the basis of all of the above results, a low redox potential of  $\text{Fe}_2(\text{SO}_4)_3$  is beneficial to thinner diameter, higher conductivity, and higher crystallinity of the PANI nanowires.

**2.3. Electrical and Electronic Transport Properties.** In order to understand the electrical and electronic transport properties of the nanowires, the conductivity at room temperature and the temperature dependence of conductivity of the nanowires were measured by a four-probe method. It is found that the conductivity at room temperature is strongly affected by the  $[\text{Fe}_2(\text{SO}_4)_3]/[\text{An}]$  ratios, as shown in Figure 4. For instance, the conductivity is increased from  $2.0 \times 10^{-3}$  to  $7.9 \times 10^0$  S/cm when the  $[\text{Fe}_2(\text{SO}_4)_3]/[\text{An}]$  ratio changes from 0.5 to 3, followed by a nearly constant conductivity of  $\sim 10^0$  S/cm at  $[\text{Fe}_2(\text{SO}_4)_3]/[\text{An}]$  ratios in between 5 and 20. A similar change in doping degree with the  $[\text{Fe}_2(\text{SO}_4)_3]/[\text{An}]$  ratios is also observed. For instance, the doping degree is increased from 0.28 to 0.36 when the  $[\text{Fe}_2(\text{SO}_4)_3]/[\text{An}]$  ratio changes from 0.5 to 3, while it is mostly unchanging (0.36–0.38) as the  $[\text{Fe}_2(\text{SO}_4)_3]/[\text{An}]$  is larger than 5. Interestingly, the maximum conductivity is achieved as high as  $\sim 10^0$  S/cm that is enhanced by  $10^2$  times compared with a conductivity of  $8.2 \times 10^{-2}$  S/cm of the nanowires (150 nm in diameter) oxidized by APS. The higher conductivity of the PANI nanowires at room temperature might result from the size effect<sup>2,6,7</sup> caused by the thinner diameter ( $\sim 10$  nm).

Temperature dependence of the conductivity for both PANI oxidized by  $\text{Fe}_2(\text{SO}_4)_3$  and APS was also measured by a four-probe method, as shown in Figure 5, where the resistivity was normalized by the resistivity at 300 K represented as  $\rho(300 \text{ K})$ . It is obvious that resistivity increases with decreasing temperature, exhibiting a semiconductor behavior. However, the nanowires oxidized by  $\text{Fe}_2(\text{SO}_4)_3$  exhibit a much weaker temperature dependence than that of nanowires oxidized by APS. For example, the resistivity ratio of  $\rho(135 \text{ K})/\rho(300 \text{ K})$  is only 4.1 for the  $\text{Fe}_2(\text{SO}_4)_3$ -oxidized nanowires but 135.2 for the APS-oxidized PANI wires. Further analysis indicates that their temperature dependences of resistivity can be interpreted in terms of quasi-one-dimensional Mott variable range hopping (quasi-1D Mott VRH) model,<sup>33</sup> as shown in Figure 5b:

$$\rho(T) = \rho_0^* \exp(T_0/T)^{1/2}$$

where  $T_0 = 18/L_c^3 N(E_F) k_B$  is the characteristic Mott temperature, which can be obtained from the  $\ln \rho(T) \sim T^{-1/2}$  plot.  $L_c$  is the localization length of charge carriers,  $k_B$  is the Boltzmann constant, and  $N(E_F)$  is the density of states at the Fermi level. The value of  $T_0$  is an important parameter, which is related to the crystalline sample and the energy needed for charge carriers' hopping conduction. Usually, the smaller value of  $T_0$  indicates the higher electrical conductivity of the sample.<sup>34</sup> For the present case, the characteristic Mott temperature,  $T_0$ , calculated from Figure 5b is  $2.5 \times 10^3$  and  $3.7 \times 10^4$  K for the PANI nanowires oxidized by  $\text{Fe}_2(\text{SO}_4)_3$  and APS, respectively. This result is also consistent with the above results that the  $\text{Fe}_2(\text{SO}_4)_3$ -oxidized nanowires show higher room-temperature conductivity and weaker temperature dependence of resistivity.

### 3. Conclusions

In summary, we exposed a facial approach to self-assemble PANI nanowires with thinner diameter ( $\sim 10$  nm), higher conductivity ( $\sim 10^0$  S/cm), and higher crystallinity by using  $\text{Fe}_2(\text{SO}_4)_3$  as a binary oxidant and dopant. Binary oxidant and dopant function of  $\text{Fe}_2(\text{SO}_4)_3$  in the nanowires has been demonstrated by structural characterizations. The low redox potential of  $\text{Fe}_2(\text{SO}_4)_3$  results in a thinner diameter, higher conductivity, and smaller characteristic Mott temperature ( $T_0 = 2.5 \times 10^3$  K) of the PANI nanowires. In particular, the method not only saves hard templates and postprocess of template removal but also simplifies reagents as compared to other methods reported previously.

### 4. Experimental Section

Aniline monomer was distilled under reduced pressure. Ferric sulfate ( $\text{Fe}_2(\text{SO}_4)_3 \cdot x\text{H}_2\text{O}$ ), ammonium persulfate ( $(\text{NH}_4)_2\text{S}_2\text{O}_8$ ,

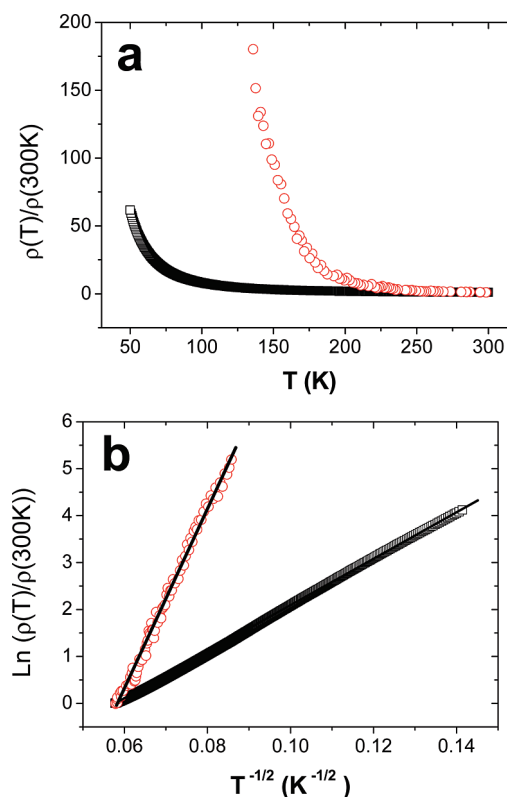


**Figure 5.** Temperature dependence of resistivity for PANI nanowires oxidized by  $\text{Fe}_2(\text{SO}_4)_3$  (black squares,  $[\text{Fe}_2(\text{SO}_4)_3]/[\text{An}] = 3:1$ ) and APS (red circles,  $[\text{APS}]/[\text{An}] = 1:1$ ): (a)  $\rho(T)/\rho(300 \text{ K})$  vs  $T$ ; (b)  $\ln[\rho(T)/\rho(300 \text{ K})]$  vs  $T^{-1/2}$ .

APS), as well as other reagents were used as received without being further treated. The PANI nanowires were self-assembled by using  $\text{Fe}_2(\text{SO}_4)_3$  as a binary oxidant and dopant. Typical polymerization processes are as follows: 0.2 mL (2 mmol) of aniline dissolved in 10 mL of deionized water with magnetic stirring at room temperature for 0.5 h. The precooled 10 mL of aqueous  $\text{Fe}_2(\text{SO}_4)_3$  (6 mmol) was added to the above solution. The mixture was allowed to react for 15 h at 0–5 °C. The PANI precipitate was washed with water, methanol, and ether several times, respectively. Finally, the product was dried in a vacuum at room temperature for 24 h. Moreover, six different molar ratios of  $\text{Fe}_2(\text{SO}_4)_3$  to aniline, which was represented by  $[\text{Fe}_2(\text{SO}_4)_3]/[\text{An}]$  ratio, at 0.5:1, 1:1, 3:1, 5:1, 10:1, and 20:1 were used to investigate the effect of the  $[\text{Fe}_2(\text{SO}_4)_3]/[\text{An}]$  ratios on the morphology and electrical properties of the resultant PANI. The nanowires are also oxidized by APS under the same procedure in order of comparison.

Morphologies of the resultant PANI were measured with a JEOL JSM-6700F field emission scanning electron microscope (SEM). The molecular structure of the nanowires was characterized by UV–visible spectra (Hitachi UV3100) dissolved in *m*-cresol and FTIR (Bruker Tensor 27) spectra. XRD analysis was carried out on a Regaku D/max2500 diffractometer at a voltage of 40 kV and a current of 200 mA with Cu K $\alpha$  radiation ( $\lambda > 1.5406 \text{ \AA}$ ). The doping degree was measured by XPS (Bruker EQUINOX55 and ES-300 (Kratos)). The room-temperature conductivity of the compressed pellets of the nanowires was measured by a standard four-probe method using a Keithley 196 System DMM Digital Multimeter and an Advantest R1642 programmable dc voltage/current generator as the current source.

Temperature dependences of the resistivity of the nanowire pellets at a temperature of 50–300 K were measured by a four-probe method using a physical property measurement system (PPMS) (Quantum Design, U.S.). Electrical contacts were made with highly conductive silver adhesive.

**Acknowledgment.** This work was financially supported by the National Natural Science Foundation of China (No. 50573090) and special fund of State Key Joint Laboratory of Environment Simulation and Pollution Control.

## References and Notes

- (1) (a) *Handbook of Conducting Polymers*; Skotheim, T. A., Ed.; Marcel Dekker: New York, 1986 and 1998. (b) Wan, M. X. *Conducting Polymers with Micro or Nanometer Structure*; Tsinghua University Press and Springer-Verlag GmbH: Beijing, Berlin, Heidelberg, 2008. (c) Wan, M. X. Conducting Polymer Nanofibers. In *Encyclopedia of Nanoscience and Nanotechnology*; Nalwa, H. S., Ed.; American Scientific Publishers: Stevenson Ranch, CA, 2004; Vol. 2, p 153.
- (2) Martin, C. R. *Science* **1994**, 266, 1961.
- (3) (a) Cai, Z.; Lei, J.; Liang, W.; Menon, V.; Martin, C. R. *Chem. Mater.* **1991**, 3, 960. (b) Liang, W.; Martin, C. R. *J. Am. Chem. Soc.* **1990**, 112, 9666. (c) Parthasarathy, R. V.; Martin, C. R. *Chem. Mater.* **1994**, 6, 1627.
- (4) Martin, C. R.; Van Dyke, L. S.; Cai, Z.; Liang, W. *J. Am. Chem. Soc.* **1990**, 112, 8976.
- (5) Liang, W.; Martin, C. R. *J. Am. Chem. Soc.* **1990**, 112, 9666.
- (6) (a) Granström, M.; Inganäs, O. *Polymer* **1995**, 36, 2867. (b) Duchet, J.; Legras, R.; Demoustier-Champagne, S. *Synth. Met.* **1998**, 98, 113.
- (7) (a) Long, Y. Z.; Zhang, L. J.; Chen, Z. J.; Huang, K.; Yang, Y. S.; Xiao, H. M.; Wan, M. X.; Jin, A. Z.; Gu, C. Z. *Phys. Rev. B* **2005**, 71, 165412. (b) Duvail, J. L.; Long, Y. Z.; Cuenot, S.; Chen, Z. J.; Gu, C. Z. *Appl. Phys. Lett.* **2007**, 90, 102114. (c) Duvail, J. L.; Dubois, S. S.; Demoustier-Champagne, Long, Y.; Piroux, L. *Int. J. Nanotechnol.* **2008**, 5, 838.
- (8) (a) Yoon, H.; Chang, M.; Jang, J. *J. Phys. Chem. B* **2006**, 110, 14074. (b) Zhang, X.; Chan-Yu-King, R.; Jose, A.; Manohar, S. K. *Synth. Met.* **2004**, 145, 23.
- (9) Tchepournaya, I.; Vasilieva, S.; Logvinov, S.; Timonov, A.; Amadelli, D.; Bartak, R. *Langmuir* **2003**, 19, 9005.
- (10) (a) Huang, J.; Virji, S.; Weiller, B. H.; Kaner, R. B. *J. Am. Chem. Soc.* **2003**, 125, 314. (b) Huang, J.; Kaner, R. B. *J. Am. Chem. Soc.* **2004**, 126, 851.
- (11) Huang, J.; Kaner, R. B. *Adv. Mater.* **2005**, 125, 314.
- (12) Wu, C.-G.; Bein, T. *Science* **1994**, 264, 1757.
- (13) Zhang, X.; Chan-Yu-King; Jose, A.; Manohar, S. K. *Synth. Met.* **2004**, 145, 23.
- (14) Huang, J.; Kaner, R. B. *J. Am. Chem. Soc.* **2004**, 126, 851.
- (15) (a) Wei, Z.; Wan, M. *Adv. Mater.* **2002**, 14, 1314. (b) Zhang, L.; Wan, M. *Adv. Funct. Mater.* **2003**, 13, 815. (c) Zhang, Z.; Wei, Z.; Wan, M. *Macromolecules* **2002**, 35, 5937. (d) Huang, K.; Wan, M. *Chem. Mater.* **2002**, 14, 3486. (e) Zhang, L.; Long, Y.; Chen, Z.; Wan, M. *Adv. Funct. Mater.* **2004**, 14, 693.
- (16) Zhang, X.; Goux, W. J.; Manohar, S. K. *J. Am. Chem. Soc.* **2004**, 126, 4502.
- (17) Chiou, N.-R.; Epstein, A. J. *Adv. Mater.* **2005**, 17, 1679.
- (18) Qiu, H.; Wan, M. *J. Polym. Sci., Part A: Polym. Chem.* **2001**, 39, 3485.
- (19) Trchova, M.; Sydenkova, I.; Konyushenko, E. N.; Stejskal, J.; Holler, P.; Cairic-Marjanovic, G. *J. Phys. Chem. B* **2006**, 110, 9461.
- (20) MacDiarmid, A. G.; Chiang, J. C.; Halpen, M.; Huang, W. S.; Mu, S. L.; Somasli, N. L.; Wu, W.; Yaniger, S. I. *Mol. Cryst. Liq. Cryst.* **1985**, 121, 173.
- (21) Ding, H.; Shen, J.; Wan, M.; Chen, Z. *Macromol. Chem. Phys.* **2008**, 209, 864.
- (22) Zhu, Y.; He, H.; Mei, M. *Acta Polym. Sin.* **2008**, 12, 1172.
- (23) Ding, H.; Wan, M.; Wei, Y. *Adv. Mater.* **2007**, 19, 465.
- (24) (a) *CRC Handbook of Chemistry and Physics*, 62nd ed.; Weast, R. C., Ed.; CRC: Boca Raton, FL, 1982. (b) *Inorganic and Analytical Chemistry*; Guo, W. L., Ed.; Harbin Institute of Technology Press: Harbin, P. R. China, 2004.
- (25) Wei, Z.; Zhang, Z.; Wan, M. *Langmuir* **2002**, 18, 917.
- (26) Kim, B. J.; G.Oh, S.; G.Han, M.; Im, S. S. *Langmuir* **2000**, 16, 5841.
- (27) Harada, M.; Adachi, M. *Adv. Mater.* **2000**, 12, 839.
- (28) (a) Chiang, J. C.; MacDiarmid, A. G. *Synth. Met.* **1986**, 13, 193. (b) MacDiarmid, A. G.; Chiang, J. C.; Richter, A. F.; Epstein, A. J. *Synth. Met.* **1987**, 18, 285.
- (29) (a) Chen, S. A.; Lee, H. T. *Macromolecules* **1995**, 28, 2858. (b) Kim, S. G.; Kim, J. W.; Choi, H. J.; Suh, M. S.; Shin, M. J.; Jhon, M. S. *Colloid Polym. Sci.* **2000**, 78, 894. (c) Tang, J. S.; Jing, X. B.; Wang, B. C.; Wang, F. S. *Synth. Met.* **1988**, 24, 231.
- (30) Sapurina, I.; Mokeev, M.; Lavrentev, V.; Zgonnik, V.; Trchová, M.; Hlavatá, D.; Stejskal, J. *Eur. Polym. J.* **2000**, 36, 2321.
- (31) (a) Jozefowicz, M. E.; Laversanne, R.; Javadi, H. H. S.; Epstein, A. J.; Pouget, J. P.; Tang, X.; MacDiarmid, A. G. *Phys. Rev. B* **1989**, 39, 12958. (b) Zhang, L.; Wan, M.; Wei, Y. *Macromol. Rapid Commun.* **2006**, 27, 366.
- (32) Pouget, J. P.; Jozefowicz, M. E.; Epstein, A. G.; Tang, X.; MacDiarmid, A. G. *Macromolecules* **1991**, 24, 779.
- (33) (a) *Electronic processes in Noncrystalline Materials*; Mott, N. F., David, E. A., Eds.; Oxford University Press: Oxford, U.K., 1979. (b) Shklovskii, B. I.; Efros, A. L. Electronic Properties of Doped Semiconductors. In *Hopping Transport in Solids*; Pollak, M., Shklovskii, B. I., Eds.; Springer-Verlag, North-Holland, Berlin, Amsterdam, 1984 and 1990.
- (34) (a) Long, Y.; Chen, Z.; Wang, N.; Zhang, Z.; Wan, M. *Physica B* **2003**, 325, 208. (b) Long, Y.; Chen, Z.; Zheng, P.; Wang, N.; Zhang, Z.; Wan, M. *J. Appl. Phys.* **2003**, 93, 2962. (c) Long, Y.; Duvail, J.; Chen, Z.; Jin, A.; Gu, C. *Polym. Adv. Technol.* **2009**, 20, 541.

JP908847U